Easy-dispersible poly(glycidyl phenyl ether)-functionalized graphene sheets obtained by reaction of "living" anionic polymer chains

Fabienne Barroso-Bujans,*[a] Virginie M. Boucher,[a] Jose A. Pomposo,[a,b,c] Lorea Buruaga,[a] Angel Alegría[a,c] and Juan Colmenero[a,c,d]

S.1 Materials

Natural graphite (universal grade, 200-mesh, 99.9995% metal basis) was supplied by Alfa Aesar. Fuming nitric acid (>90 %), potassium chlorate (ACS reagent, ≥99 %), AQUANALTM-plus nitrate (NO_3) 1-50 mg/L, glycidyl phenyl ether (99 %) and tetrabutylammonium fluoride solution (1.0 M in THF) were purchased from Sigma-Aldrich. HPLC grade solvents (tetrahydrofuran, toluene and methanol) were purchased from Scharlab and used as received. Polystyrene (PS) with an average molecular weight of 85,000 g/mol, and a polydispersity index of 1.1 was supplied by Polymer Source.

S.2 Characterization techniques

S.2.1 Size exclusion chromatography (SEC)

SEC measurements were performed on an Agilent G-1310A liquid chromatograph equipped with high performance PLgel Mixed columns and on-line differential refractometer and multi-angle laser light scattering Wyatt detectors (Optilab-Rex and Mini-Dawn Treos, respectively). Tetrahydrofuran (flow rate of 1.0 mL/min) was used as eluent at 30 °C.

S.2.2 Nuclear magnetic resonance (NMR)

Direct pulse ^{13}C magic-angle-spinning NMR spectra were recorded using a Bruker 400 WB Plus spectrometer operating at 100.6 MHz and a 4 mm MAS probe at room temperature (about 22 °C). ^{13}C Bloch decay spectra with high-power (30 kHz) ^{1}H decoupling were recorded with spinning at 7.5 kHz, 90° pulses of 7.5 μs duration, and 6 s recycle delays.

S.2.3 Elemental analysis

Elemental analysis was performed in a Euro EA3000 Elemental Analyzer (CHNS).

[a] *Centro de Física de Materiales-Material Physics Center (CSIC-UPV/EHU), Paseo Manuel Lardizábal 5, 20018 San Sebastián, Spain. Fax: +34 94301 5800; Tel: +34 94301 8793; E-mail: fbarroso@ehu.es (F Barroso-Bujans)*
[b] *IKERBASQUE-Basque Foundation for Science, Alameda Urquijo 36, 48011, Bilbao, Spain*
[c] *Departamento de Física de Materiales, Universidad del País Vasco (UPV/EHU) Apartado 1072, 20080 San Sebastián, Spain*
[d] *Donostia International Physics Center, Paseo Manuel Lardizábal 4, 20018 San Sebastián, Spain*

S.2.4 Thermogravimetric analysis (TGA)

Dynamic thermogravimetric analysis was carried out in a TGA Q500 apparatus from TA Instruments by using a heating ramp of 10 °C/min and a constant nitrogen flow of 60 mL/min.

S.2.5 Transmision electron microscopy (TEM)

TEM measurements were performed using a high-resolution transmission electron microscope TECNAI G220 TWIN. The measurements were carried out using an accelerating voltage of 200 kV, under low dose conditions. Ultrathin sections of the samples (about 70 nm) were cut by a LEICA EM UC6 microtome equipped with a diamond knife and placed on a 400-mesh copper grid.

S.2.6 Ultraviolet-visible spectroscopy (UV-Vis)

Optical transparency was studied by collecting UV-vis spectra of films on glass substrates, by using an Agilent 8453 UV-vis spectrometer. Films were spin-coated on glass substrates from toluene solutions. A clean glass slide was used as background. Spectra were collected in a wavelength range of 350 - 1000 nm.

S.2.7 Differential scanning calorimetry (DSC)

Thermal analyses of the samples were carried out by means of a differential scanning calorimeter (DSC-Q2000) from TA-Instruments. The temperature was calibrated with melting indium. All DSC measurements were performed under nitrogen atmosphere on samples of about 5 mg placed in aluminium pans.

S.2.8 Broadband dielectric spectroscopy (BDS)

A broadband dielectric spectrometer, Novocontrol Alpha analyzer, was used to measure the complex dielectric function in the frequency range from 10^2 Hz to 10^7 Hz. The samples were placed between parallel gold-plated electrodes with a diameter of 20 mm, with Teflon spacers. The sample thickness was typically 0.1 mm. The capacitor assembly was kept in a nitrogen cryostat, with temperature stability better than ±0.1 K over the duration of the experiments. BDS measurements were carried out during isothermal frequency scans recording

the complex dielectric function every 2.5 K over the temperature range of 383-438 K.

S.3 Methods

S.3.1 Synthesis of graphene sheets from graphene oxide

Graphite was oxidized using a modified Brodie method.[1,2] Briefly, a reaction flask containing 200 mL fuming nitric acid was cooled to 0 °C for 20 min and then 10 g of graphite were added. Next, 80 g of potassium chlorate was slowly added over 1 h to avoid sudden increases in temperature and the reaction mixture was stirred for 21 h at 0 °C. The mixture was diluted in distilled water and filtered until the nitrate content of the supernatant was lower than 1 mg/L. The graphite oxide slurry was dried at 80 °C for 24 h in a vacuum oven (pressure $<$ 0.1 mbar) and stored in this oven at room temperature until use. Elemental analysis of the resulting graphite oxide showed an atomic composition of $C_8H_1O_3$. The content of oxygen is related to the presence of hydroxyl, carbonyl, carboxyl, epoxy[3,4] and lactol functional groups[5]. Graphene sheets (G) were obtained by placing the graphite oxide in a glass boat and inserting it in a quartz tube under an argon flux. This tube was inserted in a tube furnace preheated to 1000 °C. After 1 min, the tube was removed and cooled down to room temperature. The elemental atomic composition of the resulting (thermally expanded/reduced) graphene sheets was $C_8H_{0.1}O_{1.2}$ showing (as expected) a significant reduction in the amount of oxygen-containing functional groups.

S.3.2 Grafting of poly(glycidyl phenyl ether) onto graphene sheets

Living, alkoxy-terminated poly(glycidyl phenyl ether) chains were prepared by anionic polymerization of glycidyl phenyl ether (2.7 g) in bulk at 60 °C using tetrabutylammonium fluoride (5 mol%) as initiator, following a recipe previously described in the literature.[6] Degasification of reagents and solvents was performed by repeated freeze-thaw cycles. All reagents were manipulated and transferred either by distillation or under inert gas in a vacuum line. After 6 h of reaction, the polymerization medium was diluted with 3 mL of tetrahydrofuran and after that, a slurry of graphene sheets (220 mg) in THF was added at once under inert atmosphere. The grafting reaction was allowed to proceed for 20 min and then it was finished by adding methanol. The poly(glycidyl phenyl ether)-functionalized graphene (FG) sheets were separated from free poly(glycidyl phenyl ether) (PGPE) by filtration and successive extraction steps with THF. The complete removal of free PGPE was verified by monitoring the UV-Visible spectra of the filtrated THF solutions. Finally, the material was dried in a vacuum oven at 80 °C until constant weight. The amount of PGPE chains anchored to graphene sheets was estimated to be 14 wt% by means of thermogravimetric analysis (Fig. S1). The number-average molecular weight and polydispersity index of PGPE were found to be 1,900 g/mol and 1.05, respectively, as determined by size exclusion chromatography. Based on the elemental atomic composition of the graphene sheets and the PGPE molecular weight, an estimation of the number of anchored chains was performed resulting in one chain per every 1000 (graphene) carbon atoms. As a control, a physical mixture of PGPE (14 wt%) and graphene sheets was prepared by direct mixing of both components in THF and further solvent drying following an identical procedure to that of FG. The broader weight loss of this sample when compared to that obtained for chemically grafted graphene (FG) sheets suggests the presence of a different type of polymer-substrate interaction (*i.e.* physisorption versus chemical anchoring). Fig. S2 shows direct ^{13}C pulse magic-angle-spinning NMR of PGPE, graphene sheets (G) and FG sheets, which clearly exhibits the presence of bands associated to phenyl groups of PGPE chains at 110-130 ppm and 160-170 ppm.[6] This result confirms the presence of PGPE chains in FG.

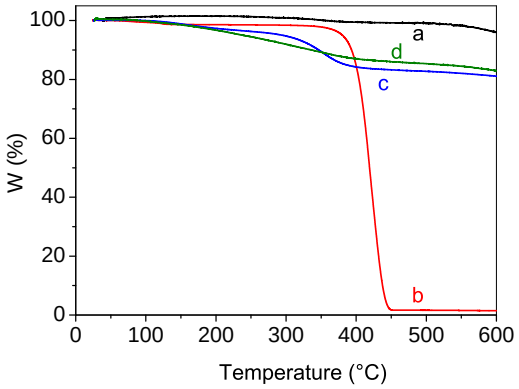

Fig. S1 A) TGA of a) graphene sheets (G), b) poly(glycidyl phenyl ether) (PGPE), c) G mixed with 14 wt% PGPE and d) chemically bonded PGPE onto G (FG), obtained at 10 °C/min in a constant nitrogen flow of 60 mL/min.

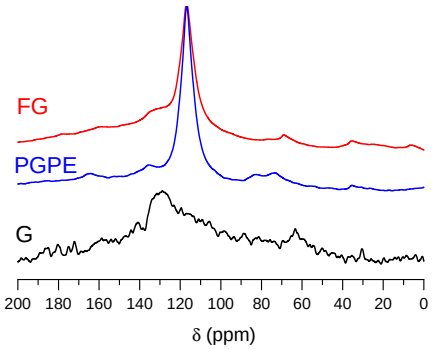

Fig. S2 Direct ^{13}C pulse magic-angle-spinning NMR for neat G, PGPE and FG.

S.3.3 Preparation of polystyrene / poly(glycidyl phenyl ether)-functionalized graphene sheet nanocomposites

A dispersion of FG sheets in toluene (0.05 g/L) was continuously stirred at 100 rpm for 15 h and finally ultrasonicated for 30 min in a water bath. Different PS / FG mixtures were subsequently prepared by adding appropriate amounts of the above solution to a solution of polystyrene in toluene (50 g/L). The resulting mixtures was then cast onto clean and warm glass substrates for fast solvent evaporation in a fume hood, followed by further evaporation of residual solvent for at least 15 h. The resulting films were finally placed in a vacuum oven at 413 K (well above the glass transition of polystyrene) for at least 72 h.

S.4 Miscellaneous

S.4.1 Optical images

The optical images of glass-supported 2.4 μm films obtained by spin coating (Fig. S3) show the presence of macrosized aggregates in PS/G composites, which disappear in the PS/FG material to give rise to a much more homogeneous and darker film. All films, PS, PS/G and PS/FG composites are optically transparent.

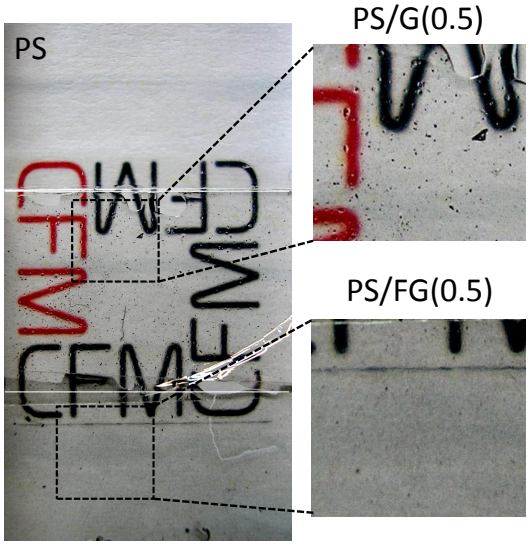

Fig. S3 Optical images of glass-supported 2.4 μm films for neat PS, PS/G and PS/FG nanocomposites with 0.5 wt% filler content as indicated in the brackets.

S.4.2 Dependence of film transparency on wavelength

No significant dependence of UV-Vis transparency on wavelength was observed for films of PS / FG nanocomposites, as illustrated in Fig. S4 for nanocomposites with a filler loading of 0.1 wt % at different film thickness.

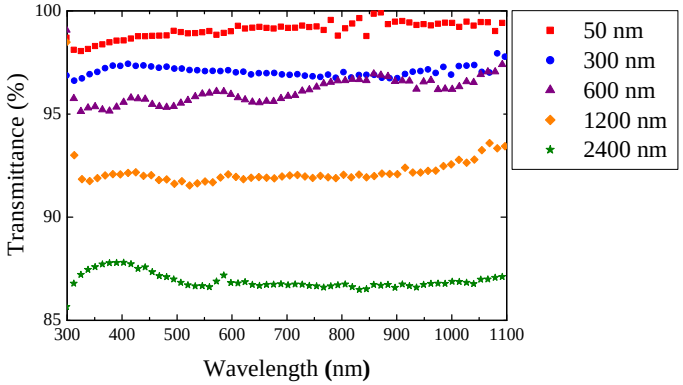

Fig. S4 Visible light transmittance spectra of PS/FG(0.1) for different film thicknesses.

S.4.3 Electrical conductivity

Table S1 Experimental values at 343 K of dc-conductivity, σ_{dc}, and time required to reach the maximum ("equilibrium") recovered enthalpy, t_{eq}, as determined by BDS and DSC, respectively, for neat PS, PS/G and PS/FG nanocomposites.

Sample	σ_{dc} (S/cm)	$\log(t_{eq})$ (s)
PS	$< 10^{-14}$	6.5
PS/G(0.1)	$< 10^{-14}$	6.1
PS/G(0.5)	$< 10^{-14}$	5.7
PS/FG(0.1)	$2.5{\cdot}10^{-13}$	5.4
PS/FG(0.5)	$3.2{\cdot}10^{-6}$	5.0

S.4.4 Comparison of polystyrene segmental dynamics in bulk and in the presence of graphene sheets

A quantitative analysis of the dielectric measurements by BDS was carried out by using the Havriliak-Negami model function (HN-function). No effect of the thermal history was found on the typical relaxation time of polystyrene, identified with the time corresponding to the maximum of the loss peak of the permittivity. From the fit of the HN-function to the data, the relaxation time τ_{HN}, the main relaxation time τ_{max}, the dielectric strength $\Delta\varepsilon$, and the shape parameters α_{HN} and γ_{HN} can be determined. Conduction effects are treated in the usual way by adding a contribution $\sigma_0/2\pi f\varepsilon_0$ to the dielectric loss, where σ_0 can be related to the specific dc-conductivity of the sample and ε_0 is the dielectric permittivity of vacuum. Another contribution to the dielectric spectrum was introduced to account for to the interfacial polarization (Maxwell/Wagner/Sillars) process, generally due to partial blocking of charge carriers at

internal surfaces or interfaces of different phases having different values of the dielectric permittivity and/or conductivity at a mesoscopic length scale or at electrodes. This process can also be fitted according to the HN function, even though it is not a molecular relaxation process. The main relaxation times of the α-process τ_{max} are plotted versus reciprocal temperature in Fig. S5 for neat polystyrene and nanocomposites of polystyrene with non-functionalized and poly(glycidyl phenyl ether)-functionalized graphene sheets.

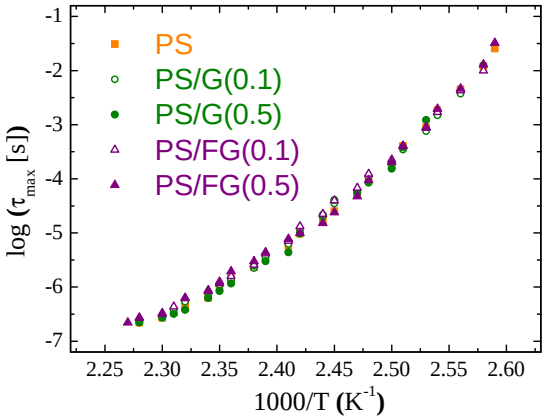

Fig. S5 Decimal logarithm of the relaxation time t_{max} versus the reciprocal temperature of pure PS, and PS/G and PS/FG nanocomposites.

S.4.5 Glass transition of polystyrene in bulk and in the presence of graphene sheets

For glass transition (T_g) measurements by DSC, all samples were first heated to 423 K and stabilized for 5 min to erase their previous thermal history, and subsequently they were cooled down at 20 K/min to room temperature for data collection. The results of T_g measurements are reported in Table S2.

Table S2 Calorimetric glass transition temperature (T_g) of neat PS, PS/G, PS/FG nanocomposites and ternary PS/G/PGPE blends.

Sample	T_g (°C)
PS	102
PS/G(0.1)	101
PS/G(0.5)	101
PS/FG(0.1)	99
PS/FG(0.5)	99
PS/G/PGPE(0.1)	101
PS/G/PGPE(0.5)	102

S.4.6 Physical aging of polystyrene in bulk and in the presence of graphene sheets

For the study of physical aging by DSC, all experiments began with a heating ramp to a temperature of 423 K, maintained for 5 min, in order to erase the material's previous thermal history. The samples were subsequently cooled down at a programmed rate of 20 K/min to reach 293 K before stabilizing at the temperature used for structural recovery, T_a, aged in the calorimeter for times from several minutes to 48 hours, before being cooled down to 293 K, at a cooling rate of 20 K/min, prior to reheating at 10 K/min for data collection. For the measurements of the enthalpy relaxation at longer aging times ($t_a > 48$ h), the annealing of the samples was carried out in an external vacuum oven, at T_a, after erasing of the thermal history and quenching of the samples in the DSC. After aging, the samples were quenched again and DSC thermograms were recorded. Second scans were run immediately after a new quench at 20 K/min. The complete thermal procedure applied to the samples for the structural recovery study has been schematized in a previous work.[7] The annealing temperatures varied in the range of 343-366 K.

The amount of enthalpy relaxed during aging (and thus recovered during DSC scan) of a glass for a period of time t_a at a given temperature T_a was evaluated by integration of the difference between the thermograms of the aged and unaged samples subsequently recorded, according to the equation:

$$\Delta H(T_a,t_a) = \int_{Tx}^{Ty} (C_p^a(T) - C_p^u(T))dT \qquad (1)$$

In this equation, C_p^a(T) and C_p^u(T) are the heat capacity measured after the annealing and that of the unannealed sample, respectively, whereas T_x and T_y are reference temperatures ($T_x < T_g < T_y$). As an example, Fig. S6 presents typical thermograms obtained for PS (as an example) after aging at T_a = 366 K. At long aging times, a plateau value of the recovered enthalpy is reached for all samples. Table S3 provides the time required to reach such a plateau, t_{eq}, at different temperatures, for neat PS, PS/G, PS/FG composites and ternary PS/G/PGPE blends.

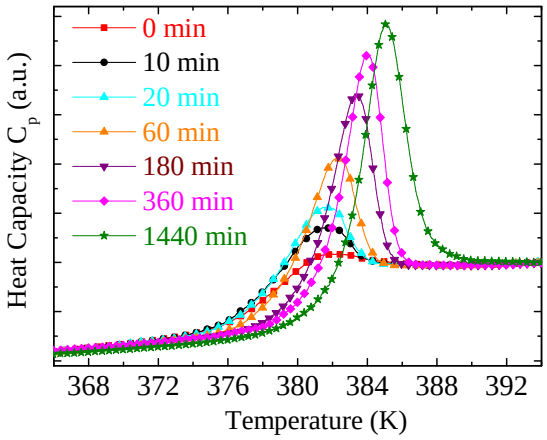

Fig. S6 DSC heating scans of pure PS, as an example, recorded after isothermal aging at T_a = 366 K, for various aging times.

Table S3 Time required to reach thermodynamical equilibrium, t_{eq}, at different aging temperatures, for PS, PS/G and PS/FG nanocomposites.

Sample	σ_{dc} (S/cm)	$\log(t_{eq})$ (s)
PS	5.6	4.7
PS/G(0.1)	5.2	4.4
PS/G(0.5)	4.8	4.0
PS/FG(0.1)	4.5	3.7
PS/FG(0.5)	4.1	3.4
PS/G/PGPE(0.1)	-	4.3
PS/G/PGPE(0.5)	-	4.0

References

S1 F. Barroso-Bujans, A. Alegría and J. Colmenero, *J. Phys. Chem. C*, 2010, **114**, 21645–21651.

S2 S. Cerveny, F. Barroso-Bujans, A. Alegría and J. Colmenero, *J. Phys. Chem. C*, 2010, **114**, 2604–2612.

S3 D. Yang, A. Velamakanni, G. Bozoklu, S. Park, M. Stoller, R. D. Piner, S. Stankovich, I. Jung, D. A. Field, C. A. Ventrice-Jr. and R. S. Ruoff, *Carbon*, 2009, **47**, 145–152.

S4 A. Bagri, C. Mattevi, M. Acik, Y. J. Chabal, M. Chhowalla and V. B. Shenoy, *Nat. Chem.*, 2010, **2**, 581–587.

S5 W. Gao, L. B. Alemany, L. Ci and P. M. Ajayan, *Nat. Chem.*, 2009, **1**, 403–408.

S6 H. Morinaga, B. Ochiai and T. Endo, *Macromolecules*, 2007, **40**, 6014–6016.

S7 V. M. Boucher, D. Cangialosi, A. Alegria and J. Colmenero, *Macromolecules*, 2010, **43**, 7594–7603.